Time-resolved detection of phase-coherent biphoton frequency combs from Si_3N_4 microring

Karthik V. Myilswamy[1,†], Mohammed S. Alshaykh[1,2,†], Hsuan-Hao Lu[1,†], Junqiu Liu[3], Daniel E. Leaird[1], Tobias J. Kippenberg[3], and Andrew M. Weiner[1,*]

[1] *School of Electrical and Computer Engineering and Purdue Quantum Science and Engineering Institute, Purdue University, West Lafayette, Indiana 47907, USA.*
[2] *Electrical Engineering department, King Saud University, Riyadh 11421, Saudi Arabia.*
[3] *Ecole Polytechnique Fédérale de Lausanne (EPFL), 1015 Lausanne, Switzerland.*

[†] *Equal contribution; *amw@purdue.edu*

Abstract: We generate a biphoton frequency comb from an integrated 40.4 GHz silicon nitride microring and probe the phase coherence through electro-optic mixing of the frequency bins followed by time-resolved detection of the time-correlation function.

Non-classical photon sources are the basic building block for emergent quantum technologies such as quantum communication and sensing as photons are robust against environmental decoherence in long-distance transmission. The advancements in photonic integrated circuits have enabled the miniaturization of both classical [1] and quantum frequency comb [2–4] and provide a route towards scalable production of quantum circuits. Of particular interest is frequency—bin entangled biphoton frequency combs (BFCs) generated in microring resonators. Encoding in the frequency domain allows versatile state manipulation with off-the-shelf telecommunication components [5], and is well-suited for high-dimensional encoding as it does not increase the system's footprint [6]. To verify the presence of entanglement, previous demonstrations [2, 3] relied on mixing different frequency modes using electro-optic phase modulators (EOM). Microrings with large free-spectral range (FSR), however, necessitated driving the EOMs at subharmonics of the FSR, increasing the unwanted scattering of frequency bins during the projection measurements. Here we report BFC generation from a silicon nitride (Si_3N_4) microring with an FSR of $\sim$ 40.4 GHz—within the range of commercial EOMs bandwidth—and modulate with a RF frequency slightly detuned from the FSR, allowing us to directly resolve the beating patterns in the time-correlation function using commercial superconducting nanowire detectors (SNSPDs) and confirm the phase coherence of the BFC state.

The Si_3N_4 microring used in the experiment was fabricated using the photonic Damascene reflow process [7] which has enabled ultra-low loss Si_3N_4 waveguides paving the way for dissipative Kerr solitons with FSRs as low as 10 GHz [1]. The spontaneous four-wave mixing arising as a consequence of third-order Kerr nonlinearity in Si_3N_4 results in a biphoton quantum state of the form $\sum_{m=1}^{\infty} \alpha_m |m,-m\rangle_{S,I}$, where $|m,-m\rangle_{S,I}$ represents the signal-idler pair which is away from the pump by $\pm m \times FSR$ and α_m is the complex probability amplitude. Fig. 1(a) depicts the experimental setup. The microring is pumped around 1550 nm using an amplified continuous-wave laser operated at a bus waveguide power of $\sim$ 15 mW, below the parametric threshold (143 mW) . The microring is overcoupled and features loaded and intrinsic Q-factors of $\sim 10^6$ and 10^7, respectively. Dense wavelength-division multiplexing filters are used before the ring to block the amplified spontaneous emission and after it to suppress the residual pump. We then use a programmable pulse shaper to select specific bins and apply spectral phase, followed by an EOM used for sideband generation. We use another pulse shaper as a wavelength selective switch to route signal and idler photons to respective SNSPDs for coincidence detection. With the EOM off, we measure the joint spectral intensity from $m = 3$ to 48 (first two pairs blocked by the filters), as shown in Fig. 1(b). Strong spectral correlations along the diagonal reflect the nature of our biphoton state. The estimated on-chip pair generation rate varies between 0.9-1.9 MHz per frequency-bin pair with a coincidences-to-accidentals of $\sim$ 40.

To further investigate the frequency-bin entanglement in the BFC state, one needs to show the phase coherence between the constituent frequency-bin pairs $|m,-m\rangle_{S,I}$. The observation of beating patterns in the time-correlation function would serve as an indicator of frequency-bin entanglement. However, the beating pattern arising from the 40.4 GHz FSR is obscured by the SNSPDs jitter ($\sim$ 80 ps), making it impossible to distinguish from the case of

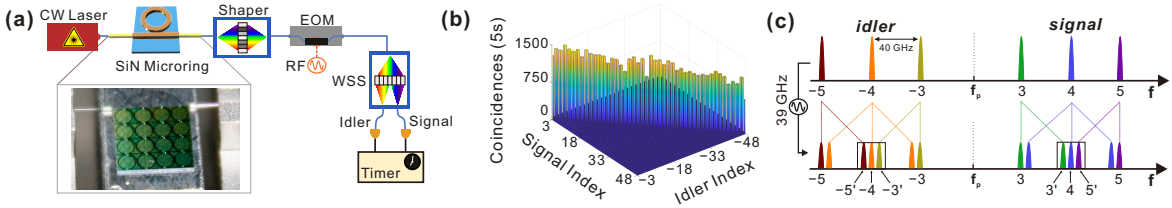

Fig. 1. (a) Experimental setup. (b) Joint spectral intensity (no accidentals subtraction). (c) Illustration of phase-modulated BFC spectrum. CW: continuous-wave. WSS: wavelength selective switch.

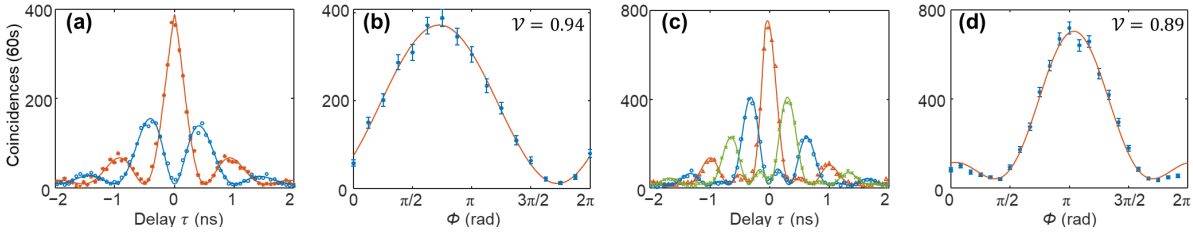

Fig. 2. Time-correlation functions for (a) $d = 2$ and (c) $d = 3$. Measured coincidences at $\tau = 0$ as a function of ϕ for (b) $d = 2$ and (d) $d = 3$. (without accidental subtraction; see text for details)

a classically correlated state. Hence, we resort to EOM to generate frequency sidebands such that the sidebands from different bins fall close to each other with a small detuning between them. For an appropriate choice of detuning, we effectively generate a new set of BFC with a smaller FSR, enabling the measurement of its time-correlation function and its probability amplitude traces the initial BFC. Our proposed scheme for up to $d = 3$ case is shown in Fig. 1(c). We pass bins $3-5$ and drive the EOM at ~ 39.4 GHz mixing all three bins around bin 4 with a detuning of 1 GHz. We then pass the photon pair around frequency mode ± 4, now consisting of contributions from neighboring bins due to phase modulation, and measure the biphoton time-correlation function. The theoretical expression for coincidence rate for this scheme, assuming all three bins have equal amplitude $\left(\alpha_m = 1/\sqrt{d}\right)$, identical Lorentzian lineshape, and are equally mixed, is given by

$$R_d(\tau) \propto e^{-\gamma|\tau|} \left| \sum_{m=1}^{d} (-1)^m e^{i(m-1)(\phi-\delta\tau)} \right|^2 \tag{1}$$

where γ denotes the photon decay rate, and τ denotes the signal-idler delay. $d = \{2,3\}$ denotes the dimensionality and δ denotes the frequency detuning between the bins after phase modulation (1 GHz in our experiments). ϕ represents the slope of the linear joint spectral phase between bin pairs applied by the pulse shaper. We have plotted the measured time-correlation functions at two different phase settings for $d = 2$ (bins $3-4$) in Fig. 2(a). We then sweep ϕ and plot the coincidences at $\tau = 0$ in Fig. 2(b). The two different phase settings in Fig. 2(a) correspond to the maximum and minimum positions of Fig. 2(b), which have a π difference between them agreeing with the theory. The plot in Fig. 2(b) has a phase offset arising due to the residual phase in the initial state, likely due to dispersion in the setup. We repeat the same experiment for bins $4-5$ to extract the phase offsets and correct for $d = 3$ case such that all three bins have equal phase to start with. We repeated the same set of experiments for $d = 3$ (bin pairs $3-5$) case and the results are plotted in Figs. 2(c-d). The phase settings for time-correlation functions shown in Fig. 2(c) correspond to the maximum ($\phi = \pi$: red) and the minimum ($\phi = \pi/3$: blue, $\phi = 5\pi/3$: green) at $\tau = 0$. In all cases, the solid curves are the theoretical predictions [Eq. 1], scaled and vertically offset to match the data points via least squares. The experimental traces are in excellent agreement with the theoretical model for both $d = 2$ and $d = 3$ cases, indeed confirming the phase coherence in our biphoton state. The visibility of the interference curves in Figs. 2(b) and (d) are higher than the classical visibility thresholds (0.71 and 0.77 for $d = 2$ and $d = 3$, respectively) and confirm the frequency-bin entanglement in the system [2, 8]. By performing an expanded set of projections, our method can be extended to reconstruct the full density matrix [9, 10].

Funding was provided by the National Science Foundation (1839191-ECCS).

References

1. J. Liu, E. Lucas, A. S. Raja, J. He, J. Riemensberger, R. N. Wang, M. Karpov, H. Guo, R. Bouchand, and T. J. Kippenberg, Nat. Photonics **14**, 486 (2020).
2. M. Kues, C. Reimer, P. Roztocki, L. R. Cortés, S. Sciara, B. Wetzel, Y. Zhang, A. Cino, S. T. Chu, B. E. Little, D. J. Moss, L. Caspani, J. Azaña, and R. Morandotti, Nature **546**, 622 (2017).
3. P. Imany, J. A. Jaramillo-Villegas, O. D. Odele, K. Han, D. E. Leaird, J. M. Lukens, P. Lougovski, M. Qi and A. M. Weiner, Opt. Express **26**, 1825 (2018).
4. M. Kues, C. Reimer, J. M. Lukens, W. J. Munro, A. M. Weiner, D. J. Moss, and R. Morandotti, Nat. Photonics **13**, 170 (2019).
5. H.-H. Lu, A. M. Weiner, P. Lougovski, and J. M. Lukens, IEEE Photon. Technol. Lett. **31**, 1858 (2019).
6. P. Imany, J. A. Jaramillo-Villegas, M. S. Alshaykh, J. M. Lukens, O. D. Odele, A. J. Moore, D. E. Leaird, M. Qi, and A. M. Weiner, npj Quantum Information **5**, 1 (2019).
7. J. Liu, A. S. Raja, M. Karpov, B. Ghadiani, M. H. P. Pfeiffer, B. Du, N. J. Engelsen, H. Guo, M. Zervas, and T. J. Kippenberg, Optica **5**, 10 (2018).
8. P. Imany, O. D. Odele, J. A. Jaramillo-Villegas, D. E. Leaird, and A. M. Weiner, Phys. Rev. A **97**, 013813 (2018).
9. R. T. Thew, K. Nemoto, A. G. White, and W. J. Munro, Phys. Rev. A **66**, 1 (2002).
10. C. Bernhard, B. Bessire, T. Feurer, and A. Stefanov, Phys. Rev. A **88**, 032322 (2013).